CHEMIJA. 2015. Vol. 26. No. 4. P. 229–237

The initial stages of copper deposition onto glassy carbon electrode modified with selenium compounds

Dijana Šimkūnaitė*,

Ignas Valsiūnas,

Vitalija Jasulaitienė,

Algirdas Selskis

State Research Institute, Center for Physical Sciences and Technology, A. Goštauto St. 9, LT-01108 Vilnius, Lithuania

The initial stages of Cu deposition onto unmodified and modified GC electrodes with selenium compounds were investigated in a 0.5 M H_2SO_4 + 0.01 M $CuSO_4$ solution over a wide range of potentials, covering both underpotential and overpotential regions. The electrochemical techniques, such as cyclic voltammetry and chronoamperometry along with structural investigation like scanning electron microscopy (SEM), X-ray photoelectron spectroscopy (XPS) and ex situ atomic force microscopy (AFM), were applied to study the nucleation and growth of Cu onto a GC electrode. On the basis of analysis of the potentiostatic current transients, it has been shown that in the potential region where Cu underpotential deposition (UPD) onto a foreign substrate is usually observed, the initial stages of Cu electrocrystallization onto the GC electrode modified with selenium compounds quite well fit the instantaneous 2D nucleation and growth model developed by Bewick et al. In the overpotential region (OPD) Cu deposition was shown to proceed by the instantaneous 3D nucleation and diffusion-controlled growth model developed by Scharifker and Hills on both the unmodified and modified with selenium compounds GC electrodes. Meanwhile, in the OPD region two successive peaked segments with the characteristic current maxima (M1 and M2) in the transients for Cu deposition onto the Se-modified GC electrode indicating some complex nucleation and growth process were determined. Some morphologic characteristics have been discussed.

Key words: copper, glassy carbon electrode, Se-modified glassy carbon electrode, underpotential deposition, overpotential deposition, early stages

INTRODUCTION

Nowadays, copper deposition is an essential process in industrial technology, especially in the field of electronics. Excellent conductive properties and the low cost of the metal have made its application favourable in almost any electronic device. On the other hand, as a constituent of important semiconductor compounds, copper has received a considerable attention concerning copper selenide layers, used mostly as solar cell materials. Nevertheless, the first reports about the appliance of copper selenides for a wide range of potential applications were published almost several decades ago, the employment of copper selenides for photovoltaic applications is still the subject of intense investigation [1–3]. A particular interest lies in cuprous selenide (Cu_2Se) that is considered a promising material for the preparation of copper indium selenide, CuInSe2, which is used for high efficient photovoltaic elements [4].

Up to date, the formation of thin copper selenide layers remains a topical issue since it is totally depended on the method of the preparation applied. A variety of techniques have been proposed for the synthesis of thin selenide films, including hot injection, vacuum evaporation, mechanical alloying, a sol–gel method, chemical bath deposition, etc. However, the electrodeposition has been the most convenient one, as it is least costly, quite effective, simple and readily adoptable when compared to most physical methods [5, 6]. It provides mild conditions for film growth and allows controlling the growth rate of the former simply by adjusting the operating parameters, such as potential or current, concentration of precursors, temperature and additives.

Generally, a simple two-step approach for the synthesis of semiconductor thin films is applied. It concerns the initial electrochemical modification of the substrate (e. g. Au) with

* Corresponding author: E-mail: nemezius@ktl.mii.lt

the chalcogen (e. g. Se^0), followed by its subsequent electroreduction in a chalcogen-free electrolyte dosed with a suitable amount of the metal ion (e. g. Cu^{2+}) [7]. A separate solution for each reactant has also been employed for the deposition of copper selenide by the so-called electrochemical atomic layer epitaxy (EC ALE) technique [8]. The former is based on the alternating electrodeposition of atomic layers of two elements at underpotentials to form a binary compound using a cycle. The cycle is repeated to achieve the desired thickness of the deposit. Ideally it is supposed that the 2-D growth mode should promote the epitaxial deposition.

Bearing in mind that modification of the substrate appears to be a necessary step in the fabrication of a semiconductor and provided that the chemical composition of the layer crucially affects the optoelectronic properties of the parent semiconductor, a possibility to control this parameter becomes of essential significance. Therefore the investigation of the initial stages (nucleation and growth) of copper electrodeposition onto a foreign substrate is of primary importance as it plays a decisive role in the film structure and properties [9]. The initial stages are usually investigated using foreign substrates, such as platinum, gold and carbon including glassy carbon (GC). In modern electroanalytical chemistry, particularly for technological use, carbon is the most common electrode material. It comes in many different forms: amorphous, crystalline-pyrolitic graphite, reticulated vitreous carbon and so forth. Although in all cases the building material is the same, carbon, it differs in its surface structure and surface properties, which influence and control its electrochemical and chemical activity [10–12]. Particular studies have been performed applying a GC electrode for its low cost, good electrical conductivity and high surface quality with excellent polishing characterizations. Nevertheless, much research has recently been carried out using modified electrodes in various electrochemical systems, and different aspects of the modification of metal electrodes by adatoms and the application of modified electrodes are discussed, but the early stages of Cu deposition onto a foreign substrate like GC in the presence of Se(IV) compounds are significantly less understood. There are only several studies in the system Cu+Se onto Se-precovered Au(poly) [7, 13] and Pt(poly) [14, 15] electrodes concerning the initial stages of copper electrocrystallization while the codeposition of Cu and Se onto various substrates and the formation of thin layers of copper selenides have been investigated extensively [16–21, 44–46]. To our knowledge, there have been no reports about the early stages of Cu electrocrystallisation onto the GC electrode modified with selenium compounds in the potential region including UPD and OPD domains so far. It should be pointed out that no Cu adlayers formation onto a stationary or rotating GC electrode has been detected during potentiodynamic Cu deposition from sulphate solutions at potentials (E_s) more positive than the equilibrium potential of a reversible Cu electrode [22]. On the other hand, in Ref. [23] the oxygen-containing surface groups of a GC electrode have been supposed to be the active centres for the discharge of Cu^{2+} ions and for the nucleation of a new phase. In the present work we reasoned to modify the GC electrode with selenium compounds that could act as the active centers for the nucleation of a new phase and to make preliminary investigations of the early stages of Cu electrodeposition onto the modified GC electrode with selenium compounds in the sulphuric acid medium, both in UPD and OPD domains.

EXPERIMENTAL

Electrochemical measurements were carried out in a conventional three-electrode cell containing 0.5 M H_2SO_4 + 0.01 M $CuSO_4$ at 20 ± 1 °C. In separate experiments, the solution containing 0.5 M H_2SO_4 + 0.01 M $CuSO_4$ + 0.05 mM H_2SeO_3 was also used. The solutions were prepared from a triply distilled water, copper sulphate (Fluka) preheated at 400 °C for 4 h, the highest purity sulphuric acid (Russia) and selenious acid (99.999% purity, Aldrich). Prior to each experiment, the working solution was deaerated with Ar gas for 0.5 h. The working electrode was a vertical disc with a diameter of 0.5 cm made from a glassy carbon rod (Sigradur G) dressed into a glass. The counter electrode was a Pt sheet of ca. 4 cm^2 in its area and the reference electrode was a Cu wire additionally coated with electrolytic Cu and immersed into the working solution. In the text, all potentials (E_s) were recalculated with respect to the standard hydrogen electrode (SHE), unless otherwise stated.

The pretreatment of the GC electrode prior to each electrochemical measurement was as follows: (i) it was mechanically polished to a nearly mirror finish with successively finer grades of alumina powders, eventually to 0.05 μm, and cleaned ultrasonically in sequence in acetone, diluted in HCl and triply distilled water; (ii) in order to obtain a clean reproducible surface before each following measurement, the GC electrode was also scanned in the background 0.5 M H_2SO_4 solution at a potential scan rate of 50 $mV \cdot s^{-1}$ for 20 min between $E_c \approx +0.25$ and $E_a \approx +1.5$ V.

The modification of the bear GC surface with thin layers of selenium compounds was performed in a 0.5 M H_2SO_4 + 0.01 M $CuSO_4$ + 0.05 mM H_2SeO_3 solution by adjusting potentiostatic pulls at a deposition potential E_{dep} = +0.28 V vs SHE at temperature 20 ± 1 °C. The consumed charge amount calculated from the integration of the applied current transient was Q = 1.25 mC cm^{-2} (with respect to the roughness factor f = 2).

For surface structural investigations, the samples were dried in an Ar stream. X-ray photoelectron spectroscopy (XPS) and Cu $L_3M_{45}M_{45}$ Auger spectroscopy (AES) analyses of the modified surface were performed using a spectrometer ESCALAB-MKII VG Scientific (UK) with an MgK_α X-ray radiation source (1253.6 eV) operated at 300 W. The pressure in the analyser chamber was maintained at 1.33×10^{-7} Pa.

Scanning electrode microscopy (SEM) and EDX analyses were performed by a scanning electron microscope EVO-50 (Carl Zeus, 2005). The samples for the ex situ atomic force

microscopy (AFM) investigations were prepared by imposing a potentiostatic pulse to a given deposition time (t_{dep}). A TopoMetrix Explorer SPM with a Si_3N_4 tip operating in a contact mode for the AFM observation was used.

The electrochemical investigations were carried out using the cyclic voltammetry and single potential step techniques. The value of E_{start} was +0.8 V. The cyclic voltammograms (CVs) and potentiostatic current-time (I/t) curves were recorded using a μAutolab Type III (Eco Chimie).

RESULTS AND DISCUSSION

To provide structural and morphological information on the GC electrode surface modified with selenium compounds SEM and XPS were performed. Figure 1 shows typical SEM images of the GC surface modified in a 0.5 M H_2SO_4 + 0.01 M $CuSO_4$ + 0.05 mM H_2SeO_3 solution by adjusting potentiostatic pulls at E_{dep} = +0.28 V. Randomly distributed irregularly-shaped particles varying from tens to hundreds nm in size are developed.

The XP spectra of the electrochemically modified GC electrode clearly confirm the presence of copper and selenium species onto the GC surface. The XPS data characterizing the surface state and elemental composition of the Se-modified GC electrode are presented in the Table and Fig. 2. The normalized content of the modified surface contains ca. 58.7 at.% of Cu, ca. 17.9 at.% of Se and ca. 23.4 at.% of oxygen. The overall elemental composition points to the formation of a discontinuous modifying layer developed after electrochemical modification of the electrode surface.

To identify different oxidation states of the mentioned elements the XP spectra were deconvoluted into several peaks centered at 932.7 and 934.7 eV for Cu $2p_{3/2}$, at 54.6 and 57.04 eV for Se $3d_{5/2}$, and at 532.1 and 533.8 eV for O 1s. The following binding energies (BE) were used as the reference BE to determine the composition of the sample surface: (i) for the Cu $2p_{3/2}$ line from Cu metallic 932.6 eV [24], from Cu_2O 932.5 eV [24], from CuO 933.7 eV, from $Cu(OH)_2$ 935.1 eV [24], from Cu_2Se 932.3 eV [25] and from CuSe 932.0 eV [26], (ii) for the Se $3d_{5/2}$ line from elemental Se 55.0 eV [25], from Cu_2Se 53.9 eV [26]. It was also taken into account that BE for O 1s in the range of ca. 532 to 533.5 or between 532.2 and 532.8 ± 0.1 eV has been previously interpreted as an adsorption of water molecules [27–30] or oxygen [31, 32] onto Cu. With regard to the selected reference BE peak centered at 932.7 eV for Cu $2p_{3/2}$ could most likely be ascribed to Cu_2O and Cu_2Se, while BE of 934.7 eV could be attributed to $Cu(OH)_2$. The Se $3d_{5/2}$ spectra centered at 54.6 eV could point to the presence of Cu_2Se in the modifying layer. Based on BE of Cu $2p_{3/2}$ spectra at 932.7 eV and Se $3d_{5/2}$ spectra at 54.6 eV, the Cu/Se mole ratio has been calculated from the height ratio of these components and it was estimated to be ca. 2:1 for the sample (i. e. Cu: Se = 36 at.%: 17.9 at.%). Such a ratio tentatively points to the development of the aforementioned compound on the surface of Se-modified GC. Nevertheless, the oxidation state of the determined

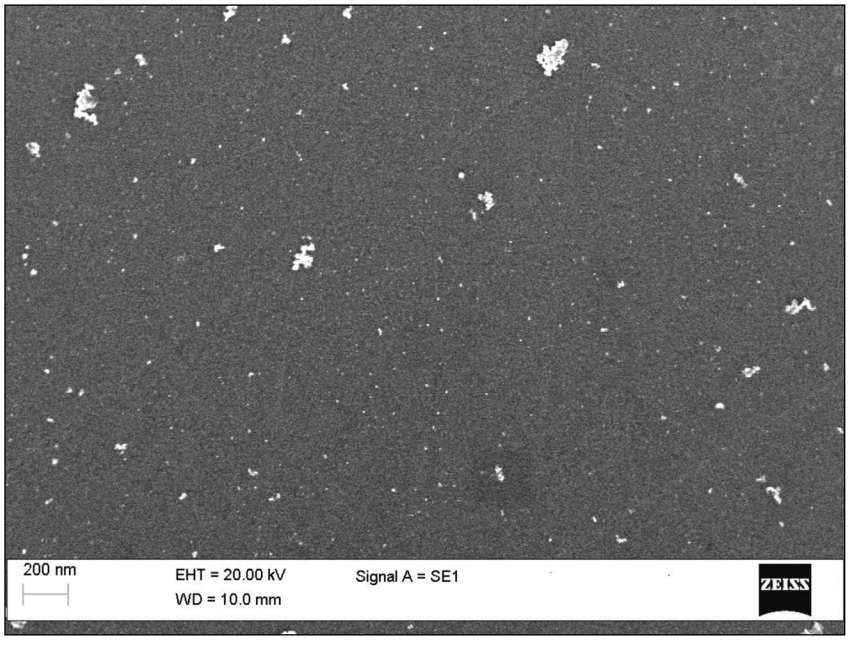

Fig. 1. SEM image of the Se-modified GC electrode obtained by adjusting potentiostatic pulls at E_{dep} = +0.28 V in 0.5 M H_2SO_4 + 0.01 M $CuSO_4$ + 0.05 mM H_2SeO_3 solution

Table. **XPS analysis of the elemental composition of the modifying layer formed on the GC surface by means of electrochemical modification**

Element	Composition, at.%	Level	Binding energy, eV	Kinetic energy, eV	Possible composition of the layer
Cu	58.71	Cu $2p_{3/2}$	932.7 and 934.7	917.5	Cu_2Se, Cu_2O, $Cu(OH)_2$, H_2O_{ads}
Se	17.9	Se $3d_{5/2}$	54.6 and 57.04		
O	23.4	O 1s	532.1 and 533.8		

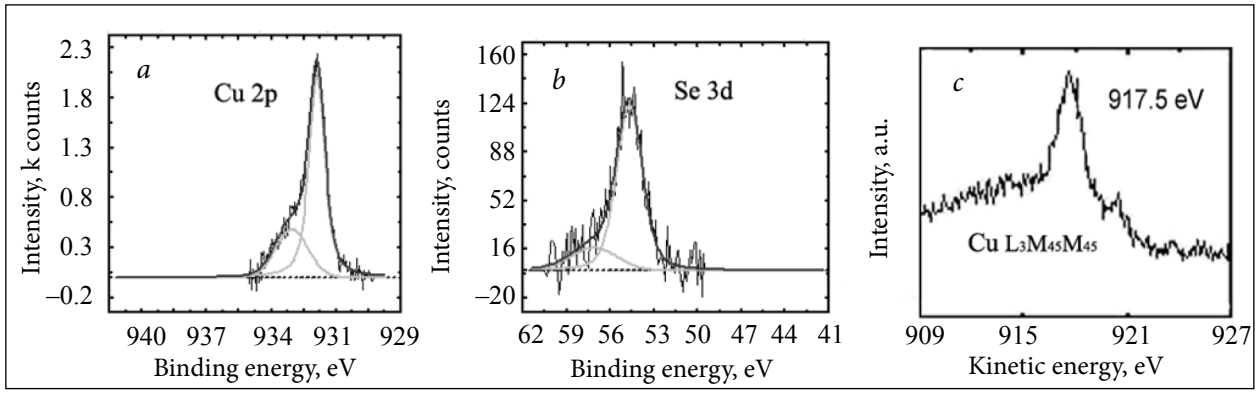

Fig. 2. Representative XP spectra for binding energies of Cu $2p_{3/2}$ (*a*) and Se $3d_{5/2}$ (*b*) and kinetic energies of Cu $L_3M_{45}M_{45}$ (*c*) for the Se-modified GC obtained by adjusting potentiostatic pulls at $E_{dep} = +0.28$ V in 0.5 M H_2SO_4 + 0.01 M $CuSO_4$ + 0.05 mM H_2SeO_3

elements is not quite obvious, however, the overall analysis of BE values denotes the most possible availability of Cu_2Se, Cu_2O, $Cu(OH)_2$ and adsorbed H_2O species in the modifying layer.

To acquire more information on the copper oxidation state the energy position of the Cu $L_3M_{45}M_{45}$ Auger region was monitored (Fig. 2c). The following AES peak energies for the Cu $L_3M_{45}M_{45}$ line were used as the reference kinetic energies (KE) for the analysis of the modifying layer: from Cu metallic 918.6 eV [24], from Cu_2O 917.2 eV [24], from CuO 918.1 eV [24], from $Cu(OH)_2$ 916.5 eV [24], from Cu_2Se 917.6 eV [26] and from CuSe 918.4 eV [26]. The one determined by us for Cu equals 917.5 eV and is rather close to that of Cu_2Se. Meanwhile, KE values for Cu metallic, CuO, CuSe differ considerably from those determined by us, therefore, are less reliable and could possibly be ruled out from the modifying layer composition.

On the other hand, it is necessary to point out some features inherent to the XP spectra interpretation. The main trouble is that we cannot exclude the oxidation by air during sample transfer and therefore the XP spectra can be influenced at least partially by oxygen. So, it is hardly possible to propose an unambiguous treatment of the results obtained. However, the values obtained and presented in the Table are rather close to the data in Ref. [33] and, analogously, could point to the fact that the surface layer is possibly composed of Cu_2Se, Cu_2O and $Cu(OH)_2$ along with the chemisorbed H_2O.

Additionally, it should be noted that the XP data are in line with the data received by the EDX data analysis, where the ration of concentrations (at.%) of separate Cu and Se elements in the modifying layer was determined to be 69:31. The assumption that the modifying layer is comprised of selenide compounds rather than of the elemental Cu and Se composition could also be supported by the fact that no Cu UPD on the unmodified GC surface has been observed by CV measurements [22]. Cyclic voltammetry was used to investigate Cu deposition onto the GC electrode modified with selenium compounds and to determine the potential region where the initial stages of copper deposition occur. Voltammetric scans were performed in potential regions between 0.80 V and –0.20 V or +0.25 V with the potential sweep initiated at 0.80 V and directed toward the negative *E* values. Figure 3 presents typical cyclic

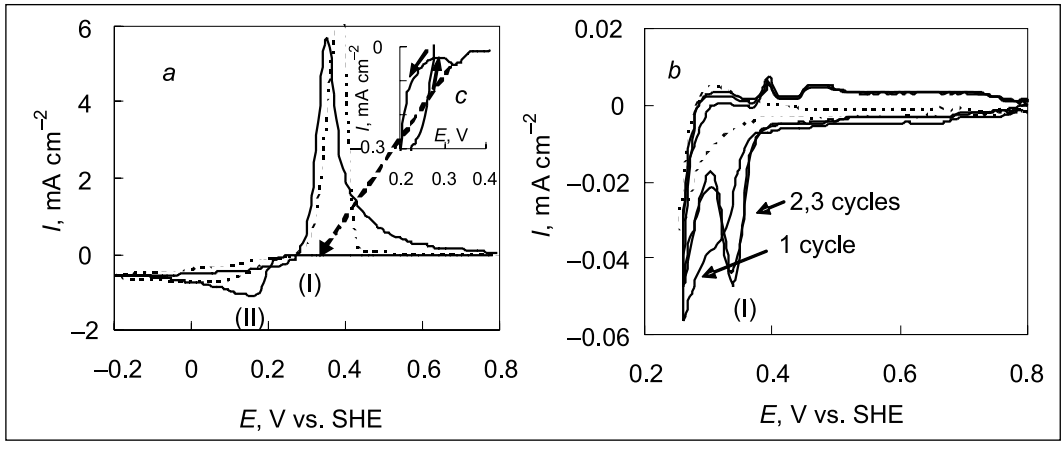

Fig. 3. Typical cyclic voltammograms for the unmodified GC (dashed line) and the Se-modified GC electrodes (solid line) in 0.5 M H_2SO_4 + 0.01 M $CuSO_4$ solution at a sweep rate of 10 mV s^{-1}, in the *E* region from $E_{start} = 0.80$ V to –0.20 V (*a*) or to +0.25 V (*b*). The inset (*c*) denotes cyclic voltammograms in the expanded scale

voltammograms for both unmodified (dotted line) and Se-modified (solid line) GC electrodes recorded in the 0.5 M H_2SO_4 + 0.01 M $CuSO_4$ solution at a sweep rate of 10 mV s^{-1}. General shapes of CVs reveal that the modification of the GC electrode results in the notably increased cathodic current with the development of two cathodic peaks in different potential domains. One peak is traditionally located in the overpotential region at *E* ca. +0.18 V (Fig. 3a), while the other one is determined in the potential region at *E* ca. +0.35 V (Figs. 3b and 3c inset) where Cu underpotential deposition is usually observed onto a foreign metal substrate. They are denoted as peaks (I) and (II) for UPD and OPD regions, respectively. It should be noted that the first current wave is not observed onto the bare GC surface under any circumstances (Fig. 3b). It develops only if the GC electrode undergoes the modification with the Se species. No Cu adlayers onto the unmodified GC surface are observed in the UPD region (Fig. 3b). Analogous results of Cu behaviour onto the bare GC in the UPD region have been determined in Ref. [22], wherein no evidence for the formation of an adatomic layer of copper has been produced. The negligible increase in the anodic current in the CV curves around the reversible *E* was supposed to be due to the oxidation of univalent copper ions accumulated in the near-electrode layer of the solution at the end of the cathodic scan of the potential rather than to the oxidation of an adatomic layer of copper [22]. Such findings point to the fact that copper underpotential deposition proceeds essentially onto the GC surface modified with selenium compounds. According to the Cu-Se phase diagram the former current peak at more positive potential (*E* ca. +0.35 V) can be related to the formation of a non-stoichiometric compound $Cu_{2-x}Se$ or stoichiometric Cu_2Se [34, 35].

However, the presence of copper adatoms at the GC surface at the very least of the cathodic overvoltages should not be completely ruled out if for no other reason than that they represent a building material for the formation of nuclei of a metallic phase [22]. The CV curves in Fig. 3a display the crossover on the reverse anodic scan over the cathodic one. The presence of the nucleation loop is a diagnostic for the formation of copper nuclei onto the GC electrode, and has been found to be indicative of the nucleation/growth process [36]. Generally, these current loops occur because the metal deposition onto a foreign substrate during cathodic scan requires a considerable overpotential in order to initiate the nucleation and subsequent growth of a deposit. Then the scan direction is reversed, the reduction faradaic current continues to flow, because the deposition of metal now takes place on the nucleated surface of substrate.

Since the evaluation of the electrocrystallization behaviour by cyclic voltammetry analysis is limited, the chronoamperometric investigations of Cu nucleation and growth onto the bare and Se-modified GC electrode were performed. Figure 4 shows a family of non-monotonic potentiostatic current-time (*I*/*t*) transients for Cu electrodeposition onto the Se-modified GC electrode for various potentials located in the region of the first current peak (I) (UPD). A set of potential steps that started from E_{start} = +0.80 V to E_{dep} between +0.34 and +0.27 V was applied. All the current transients for the Se-modified GC have a similar shape regardless of the potential used. As the potential is stepped progressively towards lower values, the increase in the current maximum (I_{max}) and the decrease in the time maximum (t_{max}) are observed. Such behaviour of transients indicates the existence of the nucleation and growth processes for all the potentials applied. However, any typical transients for the nucleation and growth of a new phase for Cu on an unmodified GC surface were not detected in the potential region of the first current peak (I).

The mechanism of nucleation and growth of a new phase onto a foreign substrate was determined by the analysis of the current transients presented in Fig. 4a on the ground

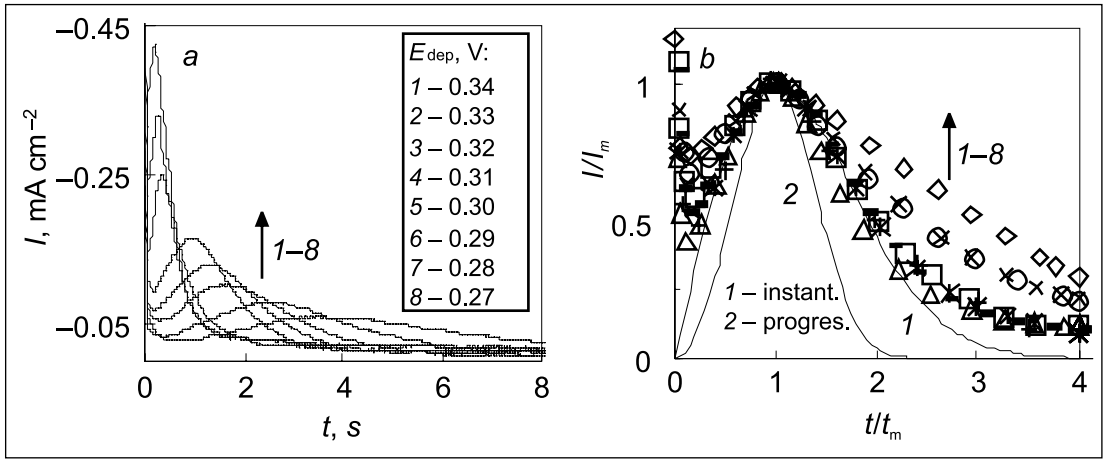

Fig. 4. (*a*) Potentiostatic current transients for the Cu electrodeposition onto the Se-modified GC electrode obtained in the UPD region by potential steps from E_{start} = +0.80 V to different deposition potentials E_{dep} in 0.5 M H_2SO_4 + 0.01 M $CuSO_4$ solution; (*b*) nondimensional plots of the potentiostatic transients in Fig. 4a. Lines: theoretical instantaneous (*1*) and progressive (*2*) 2D nucleation and growth according to the BFT model

of the theoretical model proposed by Bewick, Fleischmann and Thirsk (BFT) [37]. This model describes the kinetics of electrolytic phase formation at the early stages of 2D growth determined by the lattice incorporation of adatoms to the periphery of the growing nuclei and takes into account the overlap between neighbouring nuclei. Two limiting cases – instantaneous and progressive nucleation – have been considered by the BFT theory. They can be described in a non-dimensional form by Eqs. 1 and 2, respectively, and serve as a criterion for distinguishing between the above mentioned types of nucleation:

$$(I/I_{max}) = (t/t_{max}) \exp[-(t^2-t^2_{max}/2t^2_{max})], \quad (1)$$

$$(I/I_{max}) = (t/t_{max})^2 \exp[-2(t^3-t^3_{max}/3t^3_{max})]. \quad (2)$$

A comparison of the theoretically calculated and experimentally obtained current transients via the non-linear fitting method in Fig. 4b shows that the deposition of Cu onto the modified GC electrode with thin layers of selenium compounds in the potential region from +0.34 to +0.30 V quite well fits the instantaneous 2D nucleation and growth model developed by Bewick et al. [37]. At more negative potentials starting from +0.29 V the deviation from the instantaneous growth mode is observed.

Figure 5 shows a family of current transients for Cu electrodeposition onto the Se-modified and unmodified GC electrodes obtained at E_{dep} more negative than the equilibrium potential of a reversible Cu electrode in the region of the second current peak (II) (i. e. OPD). A set of potential steps that started from E_{start} = +0.80 V to E_{dep} between +0.10 and –0.10 V was applied. The shape of these experimental current transients for Cu deposition onto the modified GC with the selenium compounds differs significantly from those obtained onto the bare GC, as well as from those in the UPD region onto the Se-modified GC presented in Fig. 4a. Almost all experimental transients recorded at potentials more negative than +0.10 V for the Se-modified GC possess two successive peaked segments with the characteristic current maxima (M1 and M2) that merge into one at lower E_{dep} values. The presence of these segments in the chronoamperograms indicates some complex transient behaviour. Possibly, they can be described as two consecutive processes. Generally, the first current maximum at shorter times is related to 2D nucleation while the second one at longer times is related to the 3D nucleation processes. Nevertheless, 2D-2D transition via two successive monolayers prior to further 3D deposition in the OPD region was shown to be possible [43]. Anyway, all the current transients determined by us for Cu deposition on both unmodified and Se-modified GC electrodes are merging into a common curve which is caused by diffusive control and can be described by the Cottrell equation (Eq. 3):

$$I = (n\mathrm{F}D^{1/2}C_o)/(\pi^{1/2}t^{1/2}), \quad (3)$$

where I is the current density, n is the number of electrons involved in the chemical process, F is the Faraday constant, D is the diffusion coefficient, C_o is the concentration of species in the bulk and t is the time. Linearization of the experimental current transients by the means of the Cottrell equation (I vs. $1/t^{1/2}$) revealed a linear relationship clearly indicating that the copper nucleation process onto the both GC electrodes under experimental conditions was a diffusion-controlled process.

The current transients for Cu deposition onto the unmodified GC electrode (Fig. 5a) display a sharp decrease in the current at a very short time related to the double layer charging and to the occurrence of the electrochemical reaction $Cu^{2+} \rightarrow Cu$ as proposed in [38]. In fact, these transients are typical of those for the 3D nucleation and growth of a new phase at a foreign substrate surface [9]. According to the theory of Scharifker and Hills (SH model) [39], the rise in the current corresponds to the increase in the electroactive area. This increase in area, limited by a spherical diffusion around each nucleus, is accepted

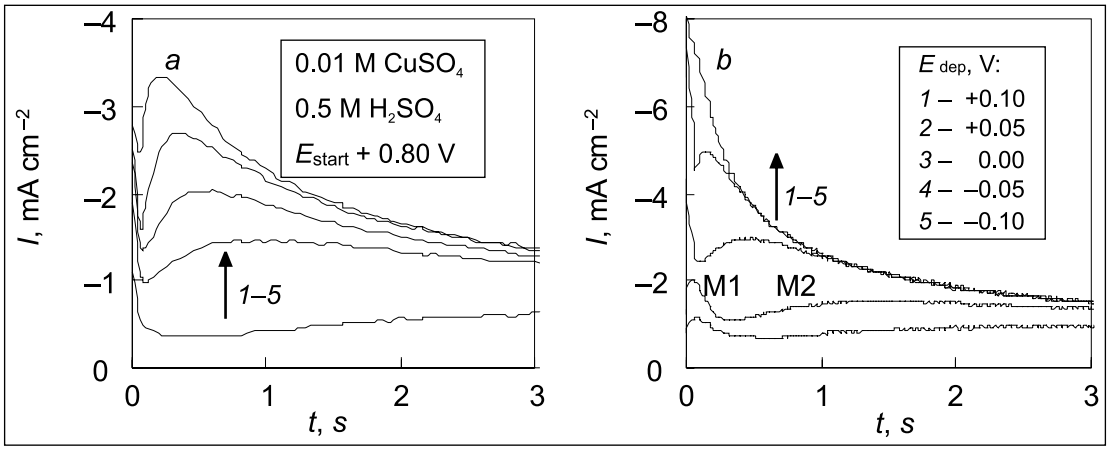

Fig. 5. Potentiostatic current transients for the Cu electrodeposition onto the bare GC electrode (*a*) and onto the Se-modified GC electrode (*b*) obtained in the OPD region by potential steps from E_{start} = +0.80 V to different deposition potentials E_{dep} in 0.5 M H_2SO_4 + 0.01 M $CuSO_4$ solution

to be due to the increase in the nucleus size and/or the increase in the number of nuclei (N). In multiple nucleations, two limiting cases that correspond to the instantaneous or progressive 3D nucleation and growth are considered. According to the SH model [39], they can be described by Eqs. 4 and 5, respectively:

$$(I/I_{max})^2 = 1.9542(t/t_{max})^{-1}\{1-\exp[-1.2564(t/t_{max})]\}^2, \quad (4)$$

$$(I/I_{max})^2 = 1.2254(t/t_{max})^{-1}\{1-\exp[-2.3367(t/t_{max})^2]\}^2. \quad (5)$$

At present, there is a considerable debate about the application of the SH model [39] or the more general one, developed by Scharifker and Mostany (SM) which allows the consideration of two extreme cases of nucleation to be eliminated, in comparison to other models proposed by other authors, e. g. Heerman and Tarallo, Sluyters-Rehbach, Mirkin and Nilov, etc. However, the SH model seems to be most commonly used to describe the early stages of metal electrocrystallization in different real systems [40]. Because of this, the SH model was applied in our work.

The experimental $(I/I_{max})^2$ vs t/t_{max} plots along with the plots calculated from Eqs. 4 and 5 are shown in Fig. 6. The fitting of experimental curves in terms of the SH model reveals that within the whole E_{dep} region applied a rather good correlation with the theoretical curve for 3D instantaneous nucleation with diffusion-controlled growth is obtained for Cu deposition onto the bare GC electrode. The analogous correlation was obtained for Se-modified Cu deposition for the second current transient maximum (M2). Nevertheless, the experimental data related to the first current transient maximum (M1) also fits the same nucleation mode (not presented), however, the analysis of the charge involved in this section of the curves amounts significantly lower to than required for the deposition of one monolayer of copper. Most likely, the current maximum at shorter times is related to the 2D nucleation rather than to 3D nucleation process. Similar potentiostatic current transients were observed in the case of Cu deposition onto the Au single crystal [41] and explained in terms of the coupled processes (i. e. adsorption, 3D nucleation) taking place simultaneously with the 2D nucleation mode for the first current maximum. On the other hand, analogous transients with two current maxima obtained for Bi nucleation on polycrystalline Pt were explained by the presence of energetically different zones on which deposition of Bi proceeds with different values of the nucleation rate [42]. Moreover, herein the inhomogeneity in different zones due to a certain accumulation of surface crystallographic defects in these zones was supposed to be of macroscopic dimensions rather than of microscopic or atomic ones.

To get more information about copper deposit onto the bare and Se-modified GC substrates ex situ AFM was used. In all cases, Cu was deposited by a single potential step from $E_{start} = 0.80$ V to $E_{dep} = -0.10$ V. The electrolysis was terminated after 10 s. The AFM images, presented in Fig. 7, show that in the case of Cu deposition onto the bare GC evenly distributed particles, rather uniform in size characterizing the instantaneous nucleation, were found. In the case of the modified GC substrate with thin layers of selenium compounds, regardless of some large particles formed, significantly smaller ones, but rather uniform in size, develop. Bearing in mind that surface modification results in the development of randomly distributed irregularly-shaped particles as is shown in Fig. 1(a), it is very likely that the deposition initially progresses exclusively at these sites. The modifying particles on the GC electrode act as the active sites or serve as the precursors for the deposition process. They are certainly distinguished by a different nature to the rest of the homogeneous surface at the same time providing energetically different conditions on different parts of the surface. Due to the presence of energetically different zones on the modified electrode substrate the nucleation and

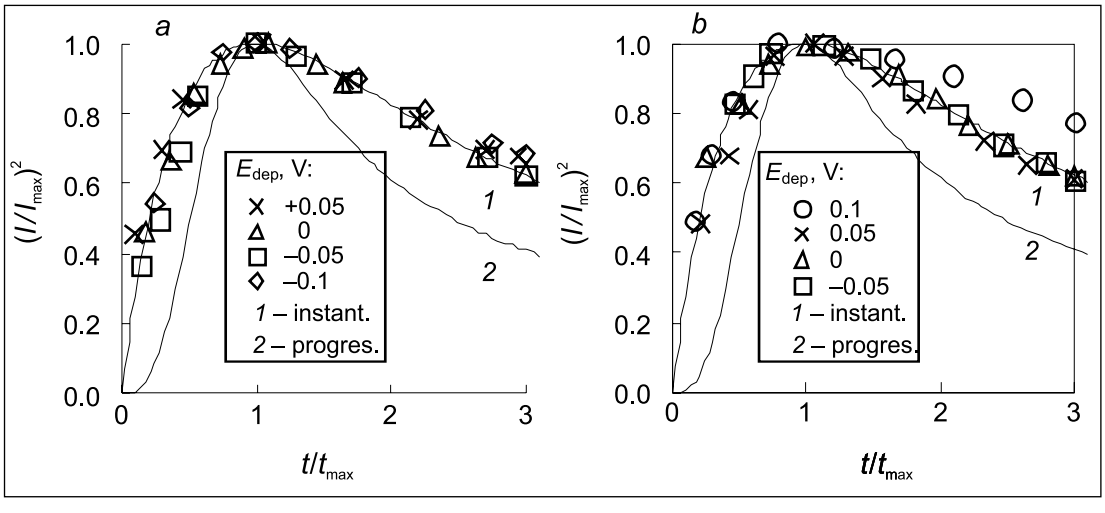

Fig. 6. Nondimensional plots of the potentiostatic transients in Fig. 5. Lines: theoretical instantaneous (*1*) and progressive (*2*) 3D nucleation and growth according to the SH model

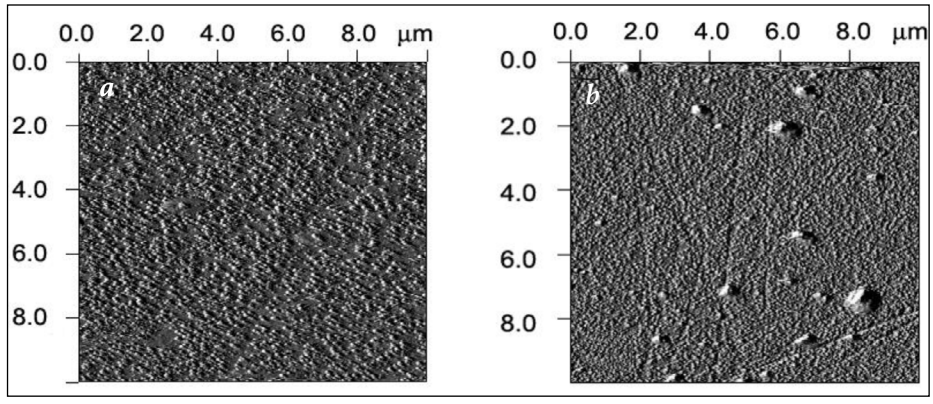

Fig. 7. Ex situ AFM image of the bare GC electrode (*a*) and the Se-modified GC electrode (*b*) after Cu electrodeposition by *E* step from $E_{start} = +0.80$ V to $E_{dep} = -0.10$ V for $t_{dep} = 10$ s from 0.5 M H_2SO_4 + 0.01 M $CuSO_4$ solution

growth of Cu observed here could proceed by different pathways (2D, 3D nucleation) and even simultaneously (i. e. overlap), finally resulting in successive peaked segments in current transients (Fig. 5b). At the early stages of Cu deposition most likely the 2D nucleation process (associated with the M1) and 3D nucleation process (associated with the M2) probably take place preferentially on the GC surface covered with selenium compounds. If the GC surface is not modified with selenium compounds, only evenly distributed particles are observed at the AFM images (Fig. 7a) and only the 3D process associated with the one current transient maximum in the *E* region under study is observed. This supposition can be partially supported by the fact that no evidence for the formation of an adatomic layer of Cu onto the bare GC electrode in the UPD region has been detected. Since the data obtained for copper deposition onto the GC modified with selenium compounds in both the UPD and OPD regions, to our knowledge, for the first time and the transients detected indicate some complex transient behaviour, the data carry only a preliminary character. In order to define real characteristics of the Cu nucleation and growth process, the influence of the neighbouring processes should be taken into account and further investigations remain to be studied additionally. Fuller examinations focused on this point are underway and will be reported in our next papers.

CONCLUSIONS

In this paper the initial stages of Cu electrodeposition onto the unmodified and modified with selenium compounds GC electrodes were investigated in a 0.5 M H_2SO_4 + 0.01 M $CuSO_4$ solution over a wide range of potentials, covering both UPD and OPD regions.

The surface analysis indicates the presence of copper and selenium species onto the electrochemically modified GC electrode. With respect to the estimated BE values it is supposed that the modifying layer most is possibly composed of Cu_2Se, Cu_2O and $Cu(OH)_2$ along with the chemisorbed H_2O.

The modification of the GC electrode was shown to result in the development of two cathodic peaks in cyclic voltammograms in different potential domains related to the underpotential and overpotential deposition of copper.

The analysis of the potentiostatic current transients in the potential region of the first current peak (I), where Cu UPD onto a foreign substrate is usually observed, reveals that the initial stages of Cu electrocrystallization onto the GC electrode modified with selenium compounds occur through the instantaneous 2D nucleation and growth model developed by Bewick et al. However, no typical transients for the nucleation and growth of a new phase for Cu on the unmodified GC surface in the potential region of the first current peak (I) were detected.

The analysis of current-time characteristics for the deposition of Cu in the OPD region on both the unmodified and modified with selenium compounds GC electrodes shows that they can be interpreted by the instantaneous 3D nucleation and diffusion-controlled growth of Cu nuclei in accordance with the model proposed by Scharifker and Hills. Meanwhile, two successive peaked segments with the characteristic current maxima (M1 and M2) in the transients for Cu deposition onto the Se-modified GC electrode in the OPD region indicate some complex nucleation and growth process, occurring via two different pathways, most possibly relating to the 2D and 3D nucleation mode. Ex situ AFM observations complement the electrochemical data and clearly show that Cu deposits on the bare and Se-modified GC electrodes possess different surface morphological characteristics and could provide some possible explanation for the origin of the nucleation process.

Received 14 July 2015
Accepted 5 October 2015

References

1. N. Moloto, H. Puggens, S. Govindraju, B. Rakgalakane, M. Kalenga, *Thin Solid Films*, **531**, 446 (2013).
2. J. Y. Lee, S. Y. Park, T. J. Lee, S. O. Ryu, *J. Nanosci. Nanotechnol.*, **13**, 2391 (2013).

3. Y. Zhao, C. Burda, *Energy Environ. Sci.*, **5**, 5564 (2012).
4. D. Chen, D. Wang, *Phys. Status Solidi A*, **10**, 2415 (2011).
5. I. M. Dharmadasa, J. Haig, *J. Electrochem. Soc.*, **153**, G47, (2006).
6. T. S. Olson, P. Antanassov, D. A. Brevnov, *J. Phys. Chem.* B, **109**, 1243 (2005).
7. W. Lee, N. Myung, K. Rajeshwar, C. W. Lee, *J. Electrochem. Sci. Technol.*, **140**, 4 (2013).
8. M. Bouroushian, *Electrochemistry of Metal Chalcogenides*, Springer-Verlag Berlin Heidelberg (2010).
9. E. Budevski, G. Staikov, W. J. Lorenz, in: *Electrochemical Phase Formation and Growth*, VCH, Weinheim (1996).
10. E. W. Linden, J. W. Dieker, *Anal. Chim. Acta.*, **119**, 1 (1980).
11. L. J. Kelpy, A. J. Bard, *Anal. Chem*., **60**, 1459 (1988).
12. R. L. McCreery, in: A. J. Bard (ed.), *Electroanalytical Chemistry. A Series of Advances*, Vol. 17, Marcel Dekker, New York, 221 (1991).
13. G. Riveros, R. Henriquez, R. Córdova, R. Schrebler, E. A. Dalchiele, H. Gómez, *J. Electroanal. Chem*., **504**, 160 (2001).
14. A. Steponavičius, D. Šimkūnaitė, *Rus. J. Electrochem*., **38**(5), 488 (2002).
15. A. Steponavičius, D. Šimkūnaitė, *Bull. Electrochem*., **18**, 367 (2002).
16. R. N. Bhattacharya, A. M. Fernandez, M. A. Contreras, et al., *J. Electrochem. Soc*., **143**, 854 (1996).
17. D. Lippkow, H.-H. Strehblow, *Electrochim. Acta*, **43**, 2131 (1998).
18. P. Carbonnelle, L. Lamberts, *J. Electroanal. Chem*., **340**, 53 (1992).
19. S. Massaccesi, S. Sanchez, J. Vedel, *J. Electrochem. Soc*., **140**, 2540 (1993).
20. A. Marlot, J. Vedel, *J. Electrochem. Soc*., **146**, 177 (1999).
21. M. Kemell, H. Saloniemi, M. Ritala, M. Leskelä, *Electrochim. Acta*, **45**, 3737 (2000).
22. A. I. Danilov, E. B. Molodkina, Y. M. Polukarov, *Rus. J. Electrochem*., **38**, 732 (2002).
23. A. I. Danilov, E. B. Molodkina, A. A. Baitov, I. V. Pobelov, Y. M. Polukarov, *Rus. J. Electrochem*., **38**, 743 (2002).
24. G. E. Muilenberg (ed.), *Handbook of X-Ray Photoelectron Spectroscopy*, Perkin-Elmer Corp. (1979).
25. D. Cahen. P. J. Ireland, L. L. Kazmerski, F. A. Thiel, *J. Appl. Phys.*, **57**, 4761 (1985).
26. R. Romad, M. Roubin, J. P. Deloume, *J. Electron Spectrosc. Relat. Phenom.*, **13**, 229 (1978).
27. B. Millet, C. Fiaud, C. Hinnen, E. M. M. Sutter, *Corros. Sci.*, **37**, 1903 (1995).
28. E. Cano. J. Simancas, J. L. Polo, C. L. Torres, J. M. Bastidas, J. Alcolea, *Mater. Corros.*, **50**, 103 (1999).
29. W. Kautek, J. G. Gordon, *J. Electrochem. Soc.*, **137**, 2672 (1990).
30. B. G. Ateya, E. A. Ashour, S. M. Sayed, *J. Electrochem. Soc*., **141**, 71 (1994).
31. T. Robert, M. Bartel, G. Offergeld, *Surf. Sci.*, **33**, 123 (1972).
32. T. Novakov, R. Prins, *Solid State Commun.*, **9**, 1975 (1971).
33. R. Ivanauskas, V. Janickis, V. Jasulaitienė, *Cent. Eur. J. Chem*., **11**, 636 (2013).
34. K. K. Mishra, K. Rajeshwar. *J. Electroanal. Chem*., **271**, 279 (1989).
35. P. Carbonelle, L. Lamberts, *Electrochim. Acta*, **37**, 1321 (1992).
36. S. Fletcher, *Electrochim. Acta*, **28**, 917 (1983).
37. A. Bewick, M. Fleischmann, H. R. Thirsk, *Faraday Soc*., **58**, 2200 (1962).
38. A. Milchev, T. Zapryanova, *Electrochim. Acta*, **51**, 2926 (2006).
39. B. Scharifker, G. Hills, *Electrochim. Acta*, **28**, 879 (1983).
40. M. E. Hyde, R. G. Compton, *J. Electroanal. Chem*., **549**, 1 (2003).
41. E. Garfias-García, M. Romero-Romo, M. Teresa Ramírez-Silva, M. Palomar-Pardavé, *Int. J. Electrochem. Sci.*, **7**, 3102 (2012).
42. V. Kapočius, L. Gudavičiūtė, V. Karpavičienė, A. Steponavičius, *Chemija*, **12**, 125 (2001).
43. M. Arbib, B. Zhang, V. Lazarov, D. Stoychev, A. Milchev, C. Buess-Herman, *J. Electroanal. Chem*., **510**, 67 (2001).
44. D. Šimkūnaitė, A. Steponavičius, V. Jasulaitienė, E. Matulionis, *Trans. IMF*., **81**, 200 (2003).
45. D. Šimkūnaitė, E. Ivaškevič, V. Jasulaitienė, A. Steponavičius, *Bull. Electrochem*., **19**, 437 (2003).
46. A. Steponavičius, D. Šimkūnaitė, I. Valsiūnas, G. Baltrūnas, *Chemija*, **22**, 91 (2011).

Dijana Šimkūnaitė, Ignas Valsiūnas, Vitalija Jasulaitienė, Algirdas Selskis

PRADINĖS VARIO NUSODINIMO STADIJOS ANT SELENO JUNGINIAIS MODIFIKUOTO STIKLIŠKOSIOS ANGLIES ELEKTRODO

S a n t r a u k a

Taikant ciklinės voltametrijos, chronoamperometrijos ir paviršiaus struktūros metodus buvo tirtos pirmosios Cu nusodinimo stadijos ant švaraus ir seleno junginiais modifikuoto stikliškosios anglies (SA) elektrodo 0,5 M H_2SO_4 + 0,01 M $CuSO_4$ tirpale plačiame potencialų intervale, apimančiame priešvoltažio (UPD) ir viršvoltažio (OPD) sritis. Nustatyta, kad UPD srityje Cu nusodinimas ant seleno junginiais modifikuotos SA vyksta pagal momentinį 2D nukleacijos ir augimo modelį, pasiūlytą Bewick ir kt. Kita vertus, šioje potencialų srityje nusodinant Cu ant švaraus SA paviršiaus jokių transientų, būdingų naujos fazės susidarymui ir jos augimui, nebuvo nustatyta. OPD srityje Cu nusodinimas ant švaraus SA elektrodo ir ant seleno junginiais modifikuotos SA vyksta pagal momentinį 3D nukleacijos ir difuzijos kontroliuojamo augimo modelį, pasiūlytą Scharifker ir Hills. Transientuose, gautuose nusodinant Cu ant Se-modifikuoto SA paviršiaus, yra stebimi du, einantys vienas paskui kitą, pikų segmentai su būdingais srovės maksimumais (M1 ir M2), kurie rodo, kad šiuo atveju Cu nukleacijos ir augimo proceso prigimtis yra sudėtinga. Kai kurios morfologinės Cu dangų charakteristikos buvo aptartos.